Engineering and Technology Journal
Journal homepage: https://etj.uotechnology.edu.iq

Effects of Dy_2O_3 doping on physical and mechanical characteristics of B_2O_3-TeO_2-BaO glass

Saba F. Hathot[a*], **Balqees M. Al dabbagh**[a], **Haydar Aboud**[b]

[a] Applied Science Dept., University of Technology-Iraq, Alsina'a street, 10066 Baghdad, Iraq.
[b] Faculty of Science- Physics Dept., Al-Mustansiriya University, Baghdad, Iraq.
*Corresponding author Email:as.21.25@grad.uotechnology.edu.iq

HIGHLIGHTS

- Barium-boro-tellurite glasses with 0-1.25% Dy_2O_3 were made using melt-quench method
- Glasses were characterized to evaluate the effects of varying Dy_2O_3 content on properties
- Increasing Dy_2O_3 density by modifying the glass network created a more compact, connected structure
- FTIR analysis provided chemical bonding and vibration information as a function of Dy_2O_3 content
- Mechanical properties improved with increased BO bonds forming from Dy_2O_3, enhancing rigidity

ARTICLE INFO

Handling editor: Akram R. Jabur

Keywords:
Glass host; Dy_2O_3; BO; FTIR; Elastic constant

ABSTRACT

A new oxide glass host of the form (50-x) B_2O_3-25TeO_2-25BaO-xDy_2O_3 (where x was varied from 0 to 1.25 mol%) was prepared using the conventional melt-cast quenching method. The study investigated how the glasses' structural, physical, and elastic properties were affected by varying amounts of Dy_2O_3. The XRD patterns of the samples indicated that they possessed an amorphous nature. FTIR spectrum displayed the vibration mode of trigonal and bipyramidal units like TeO_3, TeO_4, BO_4, and BO_3 together with Te-O-Te and Te-O linkages, indicating bridging oxygen (BO). The observed increase in the density (from 4.535 - 4.772 gm.cm^{-3}) was ascribed to the network structure contraction. The improvement in the elastic moduli of the glasses (obtained from the measured shear and longitudinal acoustic velocity) was mainly due to Dy_2O_3 doping with higher molecular weight. Consequently, it increased the glass rigidity by forming more BO in the glass network, altering the physical and structural characteristics. The obtained rise in the Debye temperature (from 334.0107–351.383 K) and softening temperature (from 399.6075-451848 K) was due to BO-mediated changes in CN. (coordination number) of the glass network. It was shown that the mechanical and structural characteristics of the proposed glass host can be tailored by tuning the Dy_2O_3 contents. These glasses may be useful for making high-strength optical fibers.

1. Introduction

Amongst all oxide glass hosts, barium-borotellurite glasses have several distinctive characteristics suitable. A significant amount of optically active ions can be dissolved (10–50) times more than in silica; nonlinear optical properties and chemical resistance make this material an excellent choice. As a result of these unique properties, tellurite glasses are ideal for fabricating various photonic devices. Furthermore, they exhibit good thermal stability against crystallization and a low glass transition temperature [1]. Compared to silicate, borate, phosphate, or chalcogenide glass, tellurite-based glass provides better shielding, elastic, and optical properties [2]. Among the many applications of barium tellurite glasses are optical fibers, LCD projector lenses, Monitors with back projection, interference meters, Optical magnifiers, and Optical systems for photography. Adding alkali metals, rare earths, transition metals, and oxides of heavy metals into TeO_2 makes it possible to significantly increase the ability of glass forming (GFA) [2]. By disrupting the random network, glass modifiers like BaO, ZnO, and PbO can make TeO_3 units and non-bridging oxygen (NBO) more compact [3]. The occurrences of weak Te-O linkages in the tellurite host matrix make the atomic network structure more porous than silicate glass. The matchless structural characteristics of tellurite glass make it an ideal host for some rare systems. The rare-earth and heavy metals-based glassy system shows small multiphoton decay rates [4].

Conversely, the unique properties of rare-earth-doped tellurite glass systems with low-phonon cut-off enable them to be used in a variety of applications, including high dielectric constants, refractive indexes, thermal and chemical stability, and low melting and phonon cut-off points [5]. In this work, two glass formers, tellurite (TeO_2) and boron oxide (B_2O_3), are blended to achieve the best structural and physical properties. B_2O_3, as a versatile glass former, has been added to various types of materials to create specific physicochemical attributes for various practical applications. Borate glass systems have generated

http://doi.org/10.30684/etj.2024.145037.1649
Received 02 December 2023; Received in revised form 28 December 2023; Accepted 01 January 2024; Available online 12 January 2024
2412-0758/University of Technology-Iraq, Baghdad, Iraq

much research interest because of their unique coordination structures, strong bond formation tendency, excellent transparency, low melting temperature, and excellent solubility of rare earths [4]. Over time, many research studies have explored the impact of various rare-earth dopants on the physical characteristics of tellurite glass with different compositions. As an illustration, in the research conducted by Umar et al., [6]. I produced a set of glass samples by employing the conventional melt-quenching technique. I observed a substantial enhancement in their overall properties as the concentration of rare-earth ions increased. Kaur et al., [1]. The characteristics of barium-tellurite glass were investigated, focusing on their thermal and optical properties. Furthermore, the impact of doping with trivalent lanthanides (Eu^{3+}, Dy^{3+}, Er^{3+}, Y^{+3}, Lu^{+3} and Nd^{3+}) on the elastic and photoluminescence properties was evaluated [1].

Abdulbaset et al., [7] a study was carried out on the characteristics of a range of zinc-tellurite glasses. These glasses were doped with Neodymium and mixed with Ag_2O. The FTIR analysis results showed that there were two active functional groups, namely TeO_3 and TeO_4. The density and molar volume of the glass composition showed an upward trend as the amount of Nd_2O_3 in it increased. Calculations were performed to determine the elastic modulus using the measured ultrasonic velocities. Both the composition of the glass system and the presence of Nd_2O_3 were found to have an impact on the elastic moduli and density of the system. The rise in elastic moduli can be attributed to both an increase in compactness and a change in the structure of the glass system. The findings from numerous studies have consistently demonstrated that the measurement of ultrasonic velocity in various lanthanides-doped oxide glass systems can offer significant information regarding their structures and physical properties.

We have created several new oxide glasses with varying chemical compositions based on the background mentioned earlier. These glasses were made by combining (50-x) B_2O_3-25TeO_2-25BaO-xDy_2O_3 using the standard and conventional preparation of the glasses method. This study sheds light on the effects of changing the concentration of Dy_2O_3 on the network structures, physical properties, and elasticity of the glasses. The primary reason for doping Dy_2O_3 was to develop a high-performance material suitable for solid-state lasers, photonics, and optoelectronics applications. Our research showed that when Dy_2O_3 was added, the glass composition became highly ionic, increasing the rigidity of the glass and its susceptibility to devitrification.The main focus of this study is to analyze the impact of Dy_2O_3 on the structural changes, morphology of the barium boro-tellurite network, and elastic properties of the glass that has been prepared, employing ultrasonic techniques. Furthermore, X-ray diffraction patterns and FTIR spectrum analysis were conducted to provide additional evidence for the collected data. Typically, the strength of amorphous materials is closely related to their elastic moduli. Thus, we can indirectly evaluate the material's strength by analyzing the elastic properties.

This search focused on a significant contribution to understanding rare earth doping in B_2O_3-TeO_2-BaO glass compositions. The key novelty of our work lies in the systematic approach employed, revealing a clear correlation between rare earth doping and enhanced mechanical properties in the glass. This extends the applicability of our findings beyond the specific glass composition studied and establishes a valuable precedent for future research in materials science and engineering.

2. Experimental work details acknowledgment

A total of six glass samples were prepared to study their composition. These samples were made using the melt-quenching method and had a composition of (50-x) B_2O_3-25TeO_2-25BaO-xDy_2O_3. Where x represented different mol% values ranging from 0 to 1.25 high purity oxides of TeO_2 (99.99%, Aldrich), B_2O_3 (99.99%, Aldrich), BaO (99.99%), and Dy_2O_3 (99.99%, Aldrich) were homogeneously mixed and melted in a (pt crucible) in an electrical furnace (970°C) for 30 minutes. In this process, and then quenched. Later, the quenched material was thermally annealed at 350°C for 3 hrs. to reduce mechanical stress, ensuring thermal and mechanical stability. To ensure consistent and uniform surfaces, all samples underwent polishing with sandpapers before proceeding with further characterizations. For XRD Crushing, a portion of each sample was necessary to obtain a fine powder for the measurements. Toluene was utilized as an immersion liquid for density measurement, following Archimedes' principle. Table 1 presents the composition of the prepared glass and its physical characteristics. The density of the glass was determined by calculation via [8]:

$$\rho = \frac{\mathrm{wa}}{\mathrm{w}_a - \mathrm{w}_l} \times \rho(\mathrm{toluene}) \quad (1)$$

The weight of the glass in air (wa) and the weight of the glass in liquid (wl) are the variables we are considering in this context. The estimation of the “molar volume” v_m of the glasses samples was calculated via [10]:

$$v_m = \frac{M}{\rho} \quad (2)$$

(OPD) of glasses was calculated by [5]:

$$(OPD) = \frac{1000 \times N}{V_m} \quad (3)$$

The room temperature “longitudinal (υ_l)”and “shear (υ_s) velocity” in the glass sample were obtained in terms of “longitudinal modulus (L)”and “shear modulus (G)” using [7]:

$$\mathrm{L} = \rho(\upsilon_l)^2 \quad (4)$$

$$G = \rho \upsilon_s{}^2 \quad (5)$$

The bulk modulus (K) was calculated via [11]:

$$K = L - \frac{4}{3} G \quad (6)$$

The "Young's modulus (E)"and "Poisson's ratio (σ)" were estimated using [12]:

$$E = (1 + \sigma)2G \quad (7)$$

$$\sigma = \frac{(L-2G)}{2(L-G)} \quad (8)$$

The values of "Debye temperature" (θ_D), "micro-hardness" (H) and "softening temperature" (T_s) were calculated using [5] [6,13] :

$$\theta_D = \frac{h}{k} \left[\frac{3\, n\, N_A}{4\pi V_m}\right]^{1/3} U_m \quad (9)$$

where h, k, and N_A are the Plank constant, Boltzmann constant, and Avogadro number, respectively.

$$H = \frac{(1-2\sigma)E}{6(1+\sigma)} \quad (10)$$

$$T_s = \frac{M_W\, v_s^2}{c^2\, n} \quad (11)$$

where c the values of constant. The value of mean ultrasonic velocity was calculated using:

$$U_m = \left[\frac{\left(\frac{1}{v_l^3}\right)+\left(\frac{2}{v_s^3}\right)}{3}\right]^{1/3} \quad (12)$$

The thermal expansion coefficient (α_p) was evaluated via [8]:

$$\alpha_p = 23.2(v_l - 0.5745) \quad (13)$$

The value of "fractal bond connectivity" (d) was evaluated using [14]

$$d = \frac{4G}{K} \quad (14)$$

3. Details of results and discussion

The XRD profiles of the samples are displayed in Figure 1, and it can be observed that no intense Bragg's diffraction peaks are present. A wide hunch indicated the amorphous nature of all samples. Investigating the density parameter allows for exploring the various fluctuations present in glass structures [13]. Figure 2 illustrates the FESEM micrographs of selected glass samples withoutdoping (a) 0 mol%,with doping Dy_2O_3 (b) 0.25 mol%,(c) 0.5 mol% ,(d) 0.75mol% , (e) 1mol% and (f) 1.25 mol%. It showed varying particle morphology (non-spherical with sharp edges). It has been noted that as the concentration of Dy^{+3} increases, the particles undergo distortion in their shape and also experience an increase in size.most particles in the sample were with a size range of 20 - 53 µm.

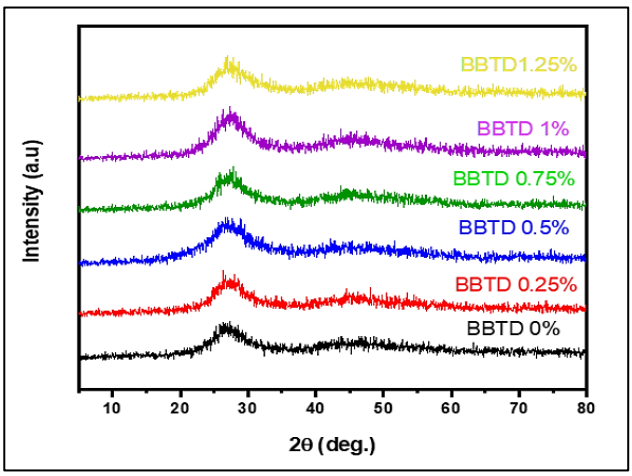

Figure 1: XRD Patterns for fabrication glasses

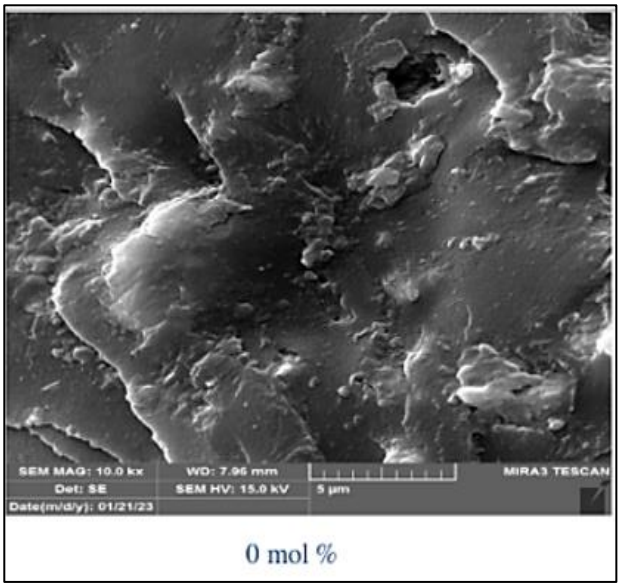

(a)

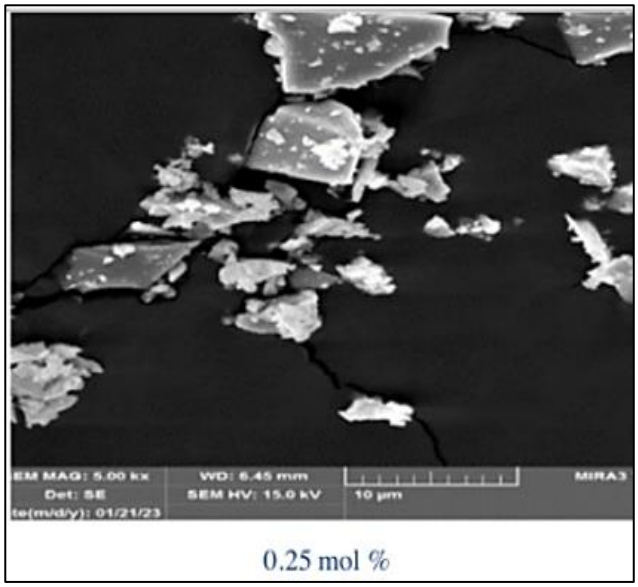

(b)

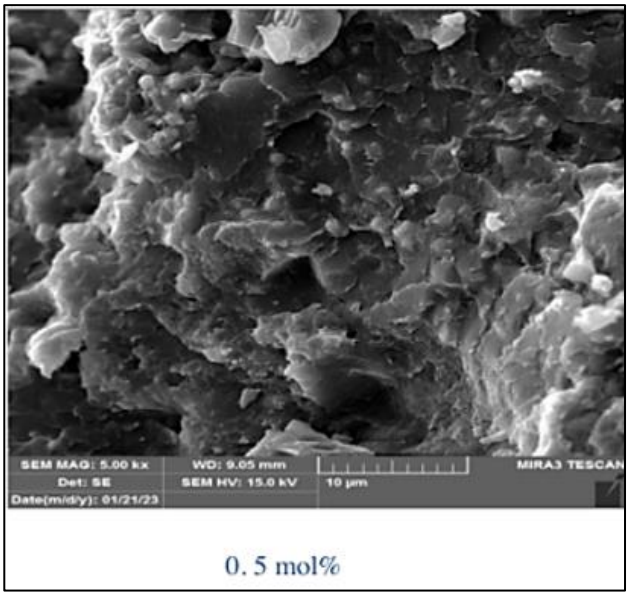

(c)

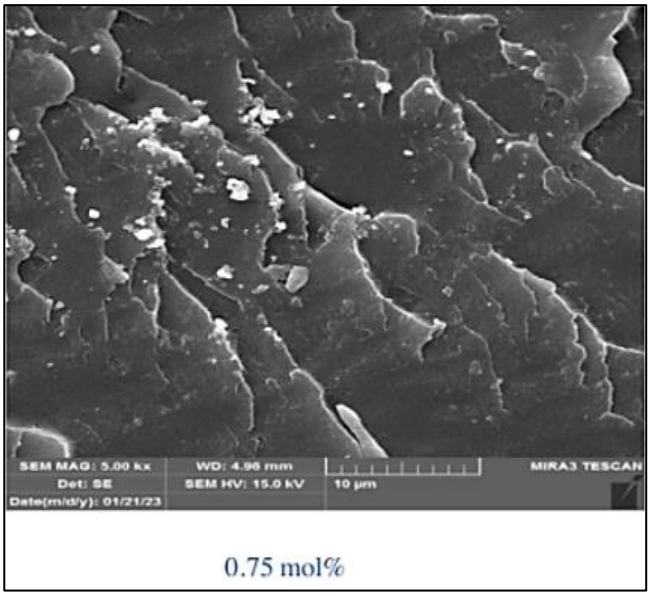

(d)

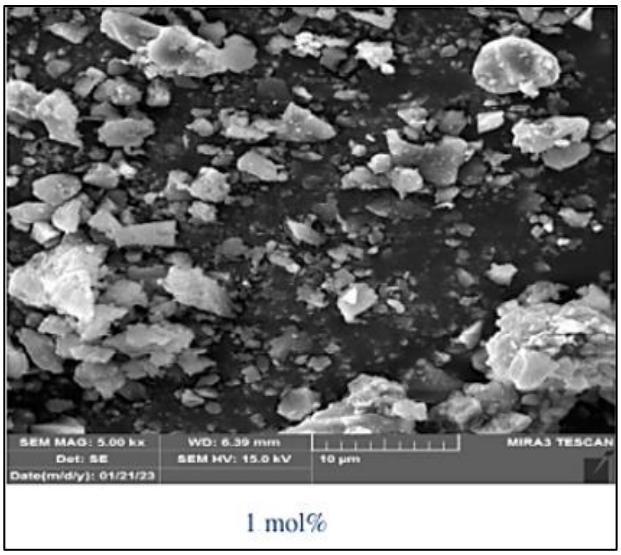

(e)

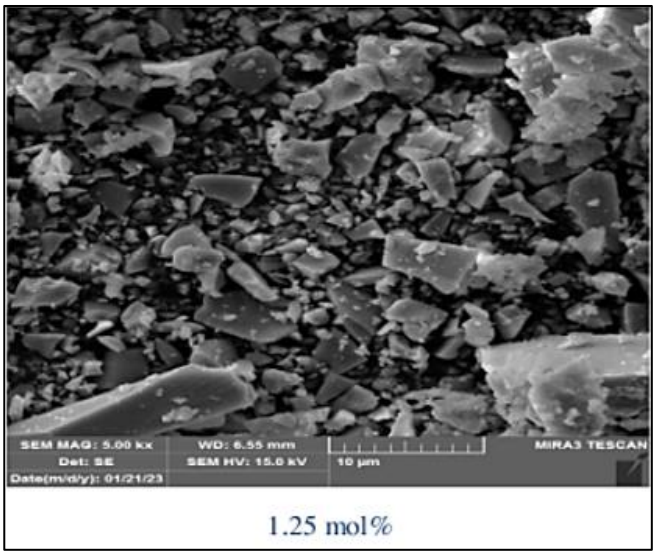

(f)

Figure 2: FESEM Images at magnification 5.00-10- Kx resolution of the glass powder without doping (a) 0 mol% with doping Dy_2O_3 (b) 0.25 mol%,(c) 0.5 mol% ,(d) 0.75mol% , (e) 1 mol% and (f) 1.25 mol%

As shown in Figure 3, the glass density values gradually rose from 4.535 to 4.772 gm/cm^3 as the concentration of Dy_2O_3 was progressively increased. Replacing the lighter B_2O_3 (69.62 amu) with the heavier Dy_2O_3 (372.9 a.m.u) could be a possible reason for the observed increase in density [15]. Moreover, the presence of Dy_2O_3 in the glass systems can affect the density increment since it modifies the glass network. This, in turn, results in a more tightly packed and interconnected glass structure [16]. The decrease in molar volume of all glass variants is depicted in Figure 4 as the concentration of Dy_2O_3 increases. One important point is that density and molar volume exhibit contrasting behaviors. An increase in Dy_2O_3 caused the molar volume of glasses to decrease from 26.493 cm^3 to 25.993 cm^3. The variations in inter-atomic spacing led to a corresponding shift in the molar volume, which can be attributed to the modifications in the structure [14]. Factors such as the length of the bond and the spacing between atoms directly influence the glass matrix and lead to a decrease in molar volume [17]. The reason that leads to a decrease in the porosity of glass is the presence of modifying ions such as Dy^{3+} at the interface sites of the glass network. [17].The number of bridging bonds in the matrix and its network determined the strength and weakening of the matrix. Glass structures become more compact as atomic ring sizes decrease, thereby decreasing molar volumes in the glass. Moreover, the cross-linking density increased, indicating increased connectivity [18]. Using oxygen packing density, a measure of how tightly the oxide network packs, it can be determined whether the oxide network is compact or not can be calculated using relation (3). Table 1 reports an increase (OPD) of 103.797 to 105.796 g. atom/l, which is connected to increasing glass density [19]. Developing more BO could make the glass network more compact, decreasing the extent of the disorder and increasing OPD [12].

Table 1: Compositions of glasses, density, molar volume, and Oxygen packing density

Composition of Glasses mol%	Sample name	ρ (g/ cm^3)	V_m (cm^3/mol)	O.P.D (gm/liter)
50 B_2O_3-25TeO_2-25BaO-0 Dy_2O_3	0%	4.535	26.493	103.797
49.75B_2O_3–25TeO_2–25BaO–0.25Dy_2O_3	0.25%	4.586	26.368	104.289
49.5B_2O_3–25TeO_2–25BaO–0.5Dy_2O_3	0.5%	4.622	26.331	104.436
49.25B_2O_3–25TeO_2–25BaO–0.75Dy_2O_3	0.75%	4.671	26.222	104.873
49.0B_2O_3–25TeO_2–25BaO–1.0Dy_2O_3	1%	4.722	26.103	105.349
48.75B_2O_3–25TeO_2–25BaO–1.25Dy_2O_3	1.25%	4.772	25.993	105.7973

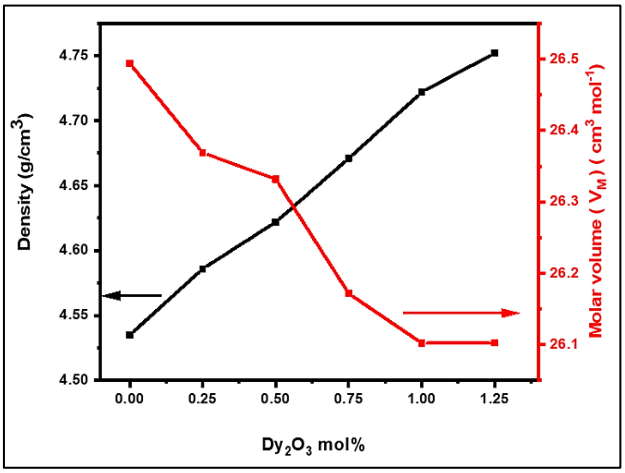

Figure 3: Density & molar volume Vs Dy_2O_3 mol% concentration

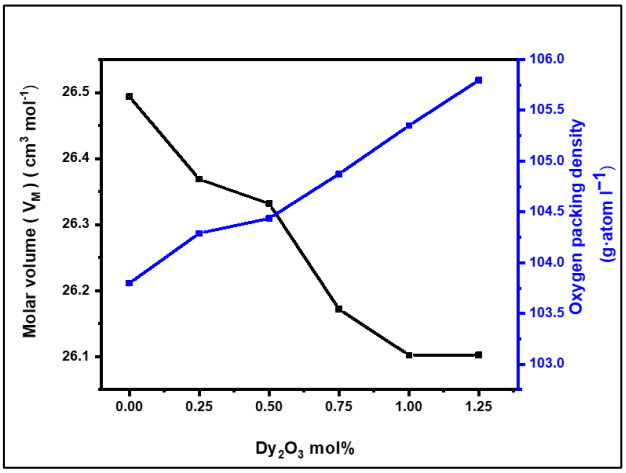

Figure 4: O.P.D & Vm of glasses of in (50-x) B_2O_3-25TeO_2-25BaO- xDy_2O_3

Figure 5 displays the FT-IR spectrum of the samples, providing information about chemical bonding and vibrations in the material as a function of Dy_2O_3 contents. Table 2 shows the locations and functions of the band in the glasses. The 464-471 cm-1 band (q^1) was caused by the vibration of the Te–O–Te bond between TeO_4 and BO [14,20]. There are three-dimensional networks of TeO_2 rich glasses that contain oxygen at two equatorial and axial sites, where only one equatorial site is connected to a lone pair electron ofTeO_4 polyhedron having 1 short and 3 extended Te-O bonds. The TeO_3 trigonal pyramid with NBO are formed when rare earth ions are integrated [21]. The bands q^2 and q^3 around 514-522 cm^{-1} and 683-692 cm^{-1} were due to axial symmetric stretching modes of TeO_4 units (tetrahedral) and (Teeq-O)s as well as (Teeq-O) vibrations of polyhedral or Tri pyramids. The observed shift in the band position from lower to higher wavenumbers in the glass matrix was related to the changes in the glass network structure [22]. There is generally a correlation between the absorption band range and emission frequency of TeO_3 trigonal pyramids (tp) [6].

A transformation of certain [TeO_3] groups into [TeO_4] groups, including BO, was indicated by the shift in the q^3 band towards lower wavenumber [23] .The band q^4 appears in the range of BaO content in the glass system, creating a new absorption peak at 1019 cm^{-1}, which may be due to the vibrations of the NBO in the form of a (BO_4) unit [16]. On the other hand, q^5 appears in the range 1414-1420 cm^{-1} assigned to stretching vibration modes of B–O linkage in BO_3 groups from different types of borate units [24]. The band q^6 appears in an area around 1572-1574 cm^{-1} and is affected by stretching vibrations of BO_3 units connected to large borate matrixes [25]. The bands q^7, q^8 and q^9 appear in the range (2934-2947,1637-1643 ,3425-3475). 2934-2947cm^{-1} was identified, which may be caused by the stretching mode of the Te-O-H groups hydrogen-bonded [26]. Band 1637-1643 cm^{-1}

assigned H-O-H [21]. 3425-3475 cm^{-1} was ascribed to OH groups [27] stretching vibration modes in water molecules [17,28]. Such vibrations may be caused by H_3BO_3 formation during sample preparation. The dysprosium oxide mode of vibration was not detected, possibly because the dopant concentration was too low for the instrument to detect [23]. Recent studies in glass science have increasingly utilized FTIR spectroscopy to gain insights into the structural characteristics of materials. FTIR provides a detailed fingerprint of molecular vibrations, offering valuable information about the arrangement of atoms in a material. More tightly packed network formation with fewer defects suggests a well-organized and ordered structure in glasses with Dy_2O_3.

Table 2: FT-IR spectral peaks positions and assignments of the fabrication glasses

Position of Bands	Band Frequency (cm^{-1})	Band Assignments	Ref.
q1	464-471	Te–O–Te bond vibration between TeO_4 and BO.	[14,20]
q2	514-522	axial symmetric stretching modes of TeO_4 units (tetrahedral) and (Teeq-O) as well as (Teeq-O) vibrations of polyhedra or tripyramids. The shift in the band position from lower to higher wavenumbers in the glass network was observed and found to be connected to changes in the glass structure.	[22]
q3	692 -683	The transformation observed involved the conversion of certain [TeO_3] groups into [TeO_4] groups that also incorporated BO.	[23]
q4	1019-1021	vibrations of NBO in the form of (BO_4) unit.	[16]
q5	1414-1420	BO_3 groups from various borate units exhibit distinct stretching vibration modes in the B–O linkage.	[24]
q6	1572-1574	stretching vibrations of BO_3 units connected to large borate matrixes.	[25]
q7	1637-1643	H-O-H	[21]
q8	2934-2947	The hydrogen-bonded Te-O-H groups exhibit a stretching mode.	[26]
q9	3425-3475	OH groups.	[27]

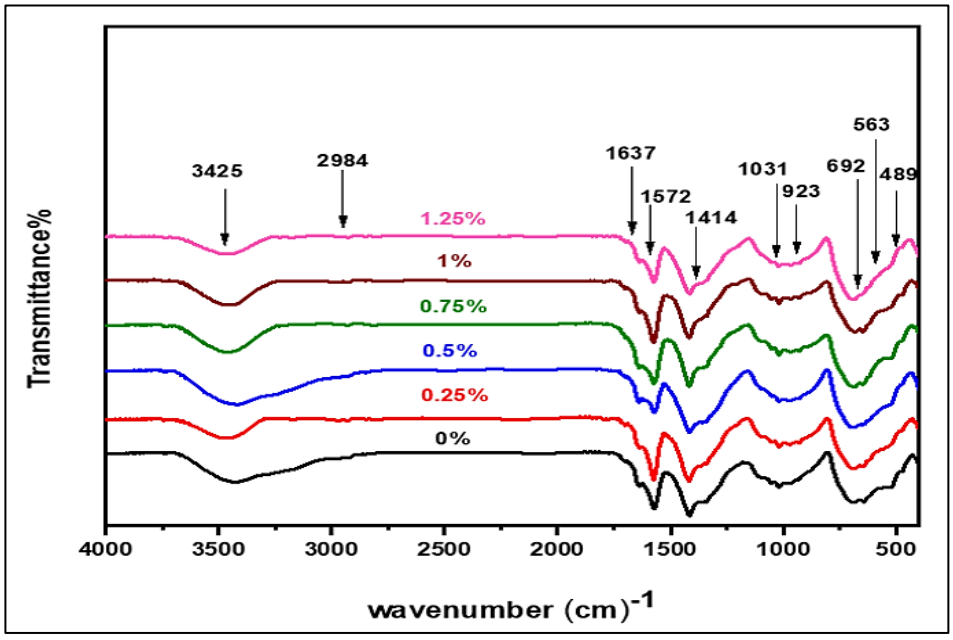

Figure 5: FT-IR Spectrum of prepared glasses

Figure 6 illustrates the impact of different quantities of Dy_2O_3 on the longitudinal and shear velocities of glasses. Figure 7 shows that different concentrations of Dy_2O_3 affect the elastic modulus of glasses. The value of ultrasonic speed was increased with the increase of Dy_2O_3 level from 0 to 1.25% Figure 6. This increase was ascribed to improving the glasses' O.P.D, bond strengths, cross-link density, and CN (coordination number) [18]. The correlation between rigidity, bond strength, BO number (TeO_4), and ultrasonic velocity was observed, indicating that as these factors increased, the resulting glass became more rigid and contained more Dy_2O_3 [29]. Reduced molar volume leads to higher ultrasonic velocities, strengthening glass [30]. Increased networking between atoms makes the glass more rigid and increases the BO number [31]. The change from TeO_3 to TeO_4 induced by Dy_2O_3 profoundly impacts the glass network's organization, [32]. This transformation leads to a more tightly packed network incorporating bridging oxygen atoms (BOs) [32]. The increase in elastic moduli, as depicted in Figure 7, is attributed to multiple factors.

One significant factor is the rise in cross-link density, which refers to the number of chemical bonds formed between the glass network. As the cross-link density increases, the glass becomes more tightly packed, and the intermolecular forces between the chains become stronger, resulting in increased rigidity. Another contributing factor is the oxygen packing density

(O.P.D), which refers to the distance that oxygen molecules can diffuse within the glass structure. When the OPD decreases, oxygen molecules are more confined within the glass, enhancing bond formation and improving material rigidity. The bond energy within the glass structure is crucial in determining its mechanical properties. Higher bond energy means stronger interactions between atoms, resulting in stiffer and more rigid glass [33]. The formation of more BO inside the glass structure improved its elastic moduli via the network structure compactness. Poisson's ratio measures the lateral and longitudinal strains. Poisson's ratio reveals the nature of a material's chemical bonding. The observed increase in the Poisson ratio value from 0.25 to 0.42 indicated an ionic bond dominance in semiconductors, glasses, and ceramics [34] conducted many studies and showed a strong relationship among the glass Poisson ratio and cross-link density (the bridging bond numbers/cation).

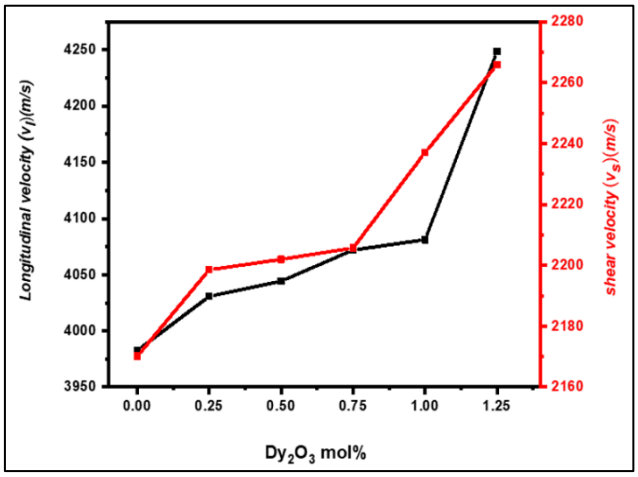

Figure 6: Longitudinal and shear velocity Vs Dy_2O_3 mol%

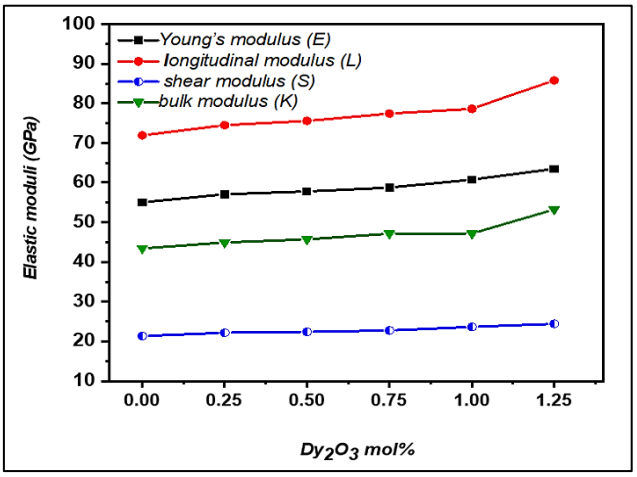

Figure 7: Elastic modulus of B_2O_3-TeO_2-BaO- Dy_2O_3 glasses

Figure 8 illustrates the variation of the Poisson ratio and Debye temperature of the glasses against Dy_2O_3 contents**.** Figure 9 depicts the effects of varying Dy_2O_3 contents on the glasses' softening temperature and thermal expansion coefficient [34]. Table 3 shows the obtained values of the Poisson ratio, micro-hardness, fractal bond connectivity, Debye temperature, softening temperature, and thermal expansion coefficient of the glasses. The progressive increase in micro-hardness in correlation with Dy_2O_3 content implies strengthening the glass structure. The rearrangement of atoms and the creation of a more rigid structure with bridging oxygen bonds contribute to this improvement in mechanical performance. The value of Debye temperature was increased mainly due to Dy^{3+} inclusion in the glass matrix, making the network more rigid [18]. Debye temperature is a significant parameter in studying solid material properties. The material's rigidity and elasticity are related to this property. Micro-hardness determined the material's resistance against permanent penetration [18]. Micro-hardness values were increased from 4.99 to 5.474 GPa as Dy_2O_3 content was increased.

TeO_3 units were transformed into TeO_4 units because bridging oxygen formed, resulting in a more compact glass structure due to the change in structural units [35]. Micro-hardness measurement indicated the deformation of a glass network via the elimination of free spaces in the glass network. The available free spaces were reduced at higher hydrostatic pressure in the glass, resulting in more compact glass network structures [32]. Viscosity is transformed into plasticity at softening temperature (Ts). The values of Ts must be correlated with the ultrasonic speed of shear waves to confirm the thermal stability of the prepared glasses [36]. With the increase of Dy_2O_3 contents Figure 9, the values of Ts were increased from 334 to 351.3 K. Improvement in the Debye and softening temperature and coefficient of thermal expansion was ascribed to the generation of more BO in the glass structure [32,37]. At room temperature, d values for prepared glasses were determined from 4G/K. With the rise of Dy_2O_3 contents, the fractal bonds in the glass series tend to get stronger. This observation was ascribed to the increasing cross-link strength between TeO_2 chains [37].

Table 3: Values of Poisson ratio, micro-hardness, fractal bond connectivity, Debye temperature, softening temperature, and coefficient of thermal expansion of (50-x) B_2O_3-25TeO_2-25BaO-x Dy_2O_3 glasses

Sample code	δ	H (GPa)	d	θ_D (k)	Ts (k)	αp
0%	0.288839	4.994241	1.966049	334.0107	399.6075	92382.5175
0.25%	0.288235	5.193470	1.972603	338.6723	413.4302	93498.1382
0.5%	0.28932	5.23227	1.960782	338.7018	420.2500	93813.163
0.75%	0.29236	5.25398	1.927931	340.9508	421.1800	94456.949
1%	0.294603	5.5886	2.005188	345.1871	437.1891	94667.752
1.25%	0.301242	5.47451	1.832936	351.3834	451.8486	98557.671

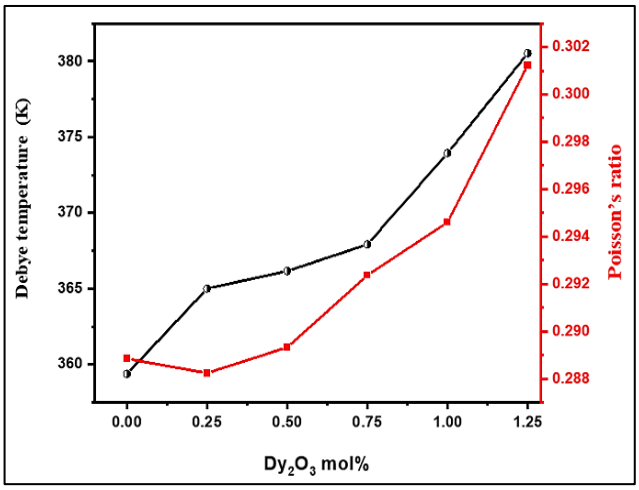

Figure 8: Poisson ratio and Debye temperature of B_2O_3-TeO_2-BaO- Dy_2O_3 glasses

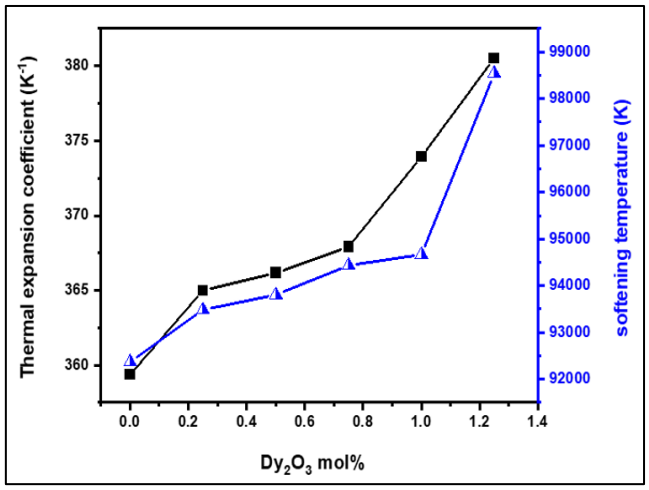

Figure 9: Softening temperature and thermal expansion coefficient of B_2O_3-TeO_2-BaO- Dy_2O_3 glasses

4. Conclusion

By utilizing melt-quenching techniques, we successfully synthesized and characterized six B_2O_3-TeO_2-BaO glass samples that were doped with different levels of Dy_2O_3. By adjusting the concentration of Dy_2O_3, it was found that the glasses' physical and mechanical properties can be tailored to meet specific requirements. Excellent transparency, thermal stability, and strong glasses were confirmed by the XRD and ultrasonic velocity measurement. Adding Dy_2O_3 to the glass systems may influence the increase in density as it modifies the glass network. As a result, the glass structure becomes more compact and connected. The molar volume of glasses decreased from 26.493 cm^3 to 25.993 cm^3 due to an increase in Dy_2O_3. Changes in the inter-atomic spacing caused a change in molar volume caused by changes in the structure.

IR spectral analysis provides information about chemical bonding and vibrations in the material and offers valuable information about the arrangement of atoms in a material. Poisson ratio and fractal bond connectivity showed that the glass structure gradually formed two-dimensional network structures, improving bond strength. Poisson's ratio reveals the nature of a material's chemical bonding. The observed increase in the Poisson's ratio value from 0.25 to 0.42 indicated an ionic bond dominance in semiconductors.

Poisson's ratio increases from 0.2888 to 0.3012. This increases the related relationship between the content of Dy_2O_3 and the enhancement of ultrasonic velocities and elastic moduli, implying a direct impact on the mechanical properties of the glass due to the formation of a greater number of bridging oxygen (BO). This study's novelty lies in the comprehensive exploration of mechanical properties in B_2O_3-TeO_2-BaO glass samples, introducing rare earth dopants at varying concentrations. Findings reveal a noteworthy enhancement in mechanical performance, including factors such as tensile strength, flexibility, and fracture resistance. This is a departure from conventional studies that may not have explored these glass compositions' full spectrum of mechanical characteristics. The connection established between oxygen bridge formation, network structure reinforcement, and subsequent improvement in mechanical performance offers exciting prospects for developing and using advanced glass materials. A deep understanding of the correlation between glass composition, structure, and mechanical properties is important for numerous industries and technology advancements. This knowledge allows the objective to enhance the strength and mechanical performance of glass materials, which will positively impact various applications.

Acknowledgment

The authors appreciate the project's assistance and encouragement from the Department of Applied Science at the University of Technology, National institute of standards cairo, Egypt and the Department of Physics, College of Science, Wasit University, Kut, Iraq.

Author contributions

Conceptualization, S. Hathor, B. Al dabbagh and H. Aboud; writing review and editing, S. Hathor; supervision, H. Aboud; project administration, B. Al dabbagh and H. Aboud. All authors have read and agreed to the published version of the manuscript.

Funding

No specific grant was obtained from any funding agency in the public, commercial, or not-for-profit sectors for this research.

Data availability statement

The data that support the findings of this study are available on request from the corresponding author.

Conflicts of interest

The authors declare that there is no conflict of interest.

References

[1] A. Kaur, A. Khanna, L.I. Aleksandrov, Structural, thermal, optical and photo-luminescent properties of barium tellurite glasses doped with rare-earth ions, J. Non-Cryst. Solids, 476 (2017) 67-74. https://doi.org/10.1016/j.jnoncrysol.2017.09.025

[2] N. Tagiara, D. Palles, E. Simandiras, V. Psycharis, A. Kyritsis, E. Kamitsos, Synthesis, thermal and structural properties of pure TeO_2 glass and zinc-tellurite glasses, J. Non-Cryst. Solids, 457 (2017) 116-125. https://doi.org/10.1016/j.jnoncrysol.2016.11.033

[3] A. Kaur, A. Khanna, C. Pesquera, F. González, V. Sathe, Preparation and characterization of lead and zinc tellurite glasses, J. Non-Cryst. Solids, 356 (2010) 864-872. https://doi.org/10.1016/j.jnoncrysol.2010.01.005

[4] P. Pawar, S. Munishwar, R. Gedam, I. white light luminescent Dy, doped lithium borate glasses for W-LED: a correlation between physical, thermal, structural and optical properties, Solid State Sci., 64 (2017) 41-50. https://doi.org/10.1016/j.solidstatesciences.2016.12.009

[5] S.F. Hathot, N.J. Jubier, R.H. Hassani, A. Salim, Physical and elastic properties of TeO_2-Gd_2O_3 glasses: Role of zinc oxide contents variation, Optik, 247 (2021) 167941. https://doi.org/10.1016/j.ijleo.2021.167941

[6] S. Umar, M. Halimah, M. Azlan, L. Grema, G. Ibrahim, A. Ahmad, A. Hamza, M. Dihom, Structural, elastic and thermo-physical properties of Er 2 O 3 nanoparticles doped bio-silicate borotellurite glasses, SN Appl. Sci., 2 (2020) 1-10. https://doi.org/10.1007/s42452-020-2112-x

[7] A. Abdulbaset, M. Halimah, S. Alazoumi, S. Umar, G. Ibrahim, Elastic properties of TeO_2–ZnO–Ag_2O doped with Nd_2O_3, Mater. Chem. Phys., 260 (2021) 124195. https://doi.org/10.1016/j.matchemphys.2020.124195

[8] M.K. Halimah, M.N.A. Hazlin, F.D. Muhammad, Experimental and theoretical approach on the optical properties of zinc borotellurite glass doped with dysprosium oxide, Spectrochim. Acta - A: Mol. Biomol. Spectrosc., 195 (2018) 128-135. https://doi.org/10.1016/j.saa.2017.12.054

[9] M. Nalin, M. Poulain, S. Ribeiro, Y. Messaddeq, Crystallization study of the (1− x) Sb_2O_3–(x) $SbPO_4$ glass system, Mater. Chem. Phys., 112 (2008) 1069-1073. https://doi.org/10.1016/j.matchemphys.2008.07.033

[10] D. Tatar, G. Özen, F. Erim, M. Öveçoğlu, Raman characterizations and structural properties of the binary TeO_2-WO_3, TeO_2- CdF_2 and ternary TeO_2- CdF_2–WO_3 glasses, J. Raman Spectrosc., 41 (2010) 797-807. https://doi.org/10.1002/jrs.2519

[11] H.A. Aziz Sidek, S. Rosmawati, M.K. Halimah, K.A. Matori, Z.A. Talib, Effect of AlF 3 on the Density and Elastic Properties of Zinc Tellurite Glass Systems, Materials, 5 (2012) 1996-1944. https://doi.org/10.3390/ma5081361

[12] N. Elkhoshkhany, R. El-Mallawany, E. Syala, Mechanical and thermal properties of TeO_2–Bi_2O_3–V_2O_5–Na_2O–TiO_2 glass system, Ceram. Int., 42 (2016) 19218-19224. https://doi.org/10.1016/j.ceramint.2016.09.086

[13] Y.B. Saddeek, N. Elsayed, Structural and mechanical features of some lanthanum tellurite glasses, Can. J. Phys., 93 (2015) 460-465. https://doi.org/10.1139/cjp-2014-0044

[14] N. Elkhoshkhany, R. Abbas, R. El-Mallawany, A. Fraih, Optical properties of quaternary TeO_2–ZnO–Nb_2O_5–Gd_2O_3 glasses, Ceram. Int., 40 (2014) 14477-14481. https://doi.org/10.1016/j.ceramint.2014.07.006

[15] F. Mohd Fudzi, H. Mohamed Kamari, A. Abd Latif, A. Muhammad Noorazlan, Linear optical properties of zinc borotellurite glass doped with lanthanum oxide nanoparticles for optoelectronic and photonic application, J. Nanomater., 2017 (2017). https://doi.org/10.1155/2017/4150802

[16] A. Rajiv, M.S. Reddy, J. Uchil, C.N. Reddy, Thermal and Optical properties of Sodium-Phospho-Zinc-Neodymium oxide glass system, J. Adv. Sci. Res., 5 (2014) 32-39.

[17] V. Kamalaker, G. Upender, C. Ramesh, V.C. Mouli, Raman spectroscopy, thermal and optical properties of TeO_2–ZnO–Nb_2O_5–Nd_2O_3 glasses, Spectrochim. Acta, Part A, 89 (2012) 149-154. https://doi.org/10.1016/j.saa.2011.12.057

[18] M. Halimah, S. Umar, K. Chan, A. Latif, M. Azlan, A. Abubakar, A. Hamza, Study of rice husk silicate effects on the elastic, physical and structural properties of borotellurite glasses, Mater. Chem. Phys., 238 (2019) 121891. https://doi.org/10.1016/j.matchemphys.2019.121891

[19] M. Mhareb, R. Alsharhan, M. Sayyed, Y. Alajerami, M. Alqahtani, T. Alayed, M. Almurayshid, The impact of TeO_2 on physical, structural, optical and radiation shielding features for borate glass samples, Optik, 247 (2021) 167924. https://doi.org/10.1016/j.ijleo.2021.167924

[20] K.F. Ahmed, S.O. Ibrahim, M.R. Sahar, S.Q. Mawlud, Effect of Rare Earth Co-Doping On Physical and Optical Characterization of Zinc Tellurite Glass Embedded Ag NPs, ZANCO J. Pure Appl. Sci., 28 (2017) 68-73.

[21] P.G. Pavani, K. Sadhana, V.C. Mouli, Optical, physical and structural studies of boro-zinc tellurite glasses, Physica B, 406 (2011) 1242-1247. https://doi.org/10.1016/j.physb.2011.01.006

[22] E.S. Yousef, A. Al-Salami, M. Hotzel, Optical and thermal characteristics of glasses based on TeO_2, Bull. Mater. Sci., 35 (2012) 961-967. https://doi.org/10.1007/s12034-012-0393-4

[23] M.A. Hazlin, M. Halimah, F. Muhammad, M. Faznny, Optical properties of zinc borotellurite glass doped with trivalent dysprosium ion, Physica B: Condens. Matter., 510 (2017) 38-42. https://doi.org/10.1016/j.physb.2017.01.012

[24] N.R. Mohamad Azaludin, N.S. Sabri, Infrared spectroscopy of mixed glass former effect in borotellurite glasses: A review, Gading J. Sci. Technol., 4 (2021) 94-102.https://ir.uitm.edu.my/id/eprint/46258

[25] N. Elkhoshkhany, N. Samir, Structural, thermal and optical properties of oxy-fluoro borotellurite glasses, J. Mater. Res.Technol., 9 (2020) 2946-2959. https://doi.org/10.1016/j.jmrt.2020.01.045

[26] M. O'Donnell, C. Miller, D. Furniss, V. Tikhomirov, A. Seddon, Fluorotellurite glasses with improved mid-infrared transmission, J. Non-Cryst. Solids, 331 (2003) 48-57. https://doi.org/10.1016/j.jnoncrysol.2003.08.081

[27] K. Nanda, N. Berwal, R. Kundu, R. Punia, N. Kishore, Effect of doping of Nd3+ ions in $BaO–TeO_2–B_2O_3$ glasses: A vibrational and optical study, J. Mol. Struct., 1088 (2015) 147-154. https://doi.org/10.1016/j.molstruc.2015.02.021

[28] S. Ghoshal, A. Awang, M. Sahar, R.J. Amjad, M.R. Dousti, Spectroscopic and structural properties of TeO_2-ZnO-Na_2O-Er2O3-Au glasses, Chalcogenide Lett., 10 (2013) 411-420.

[29] S. Alazoumi, H. Sidek, M. Halimah, K. Matori, M. Zaid, A. Abdulbaset, Synthesis and elastic properties of ternary ZnO-PbO-TeO_2 GLASSES, Chalcogenide Lett., 14 (2017) 1841-4834.

[30] Y.B. Saddeek, H. Afifi, N. Abd El-Aal, Interpretation of mechanical properties and structure of $TeO_2–Li_2O–B_2O_3$ glasses, Phys. B: Condens. Matter, 398 (2007) 1-7. https://doi.org/10.1016/j.physb.2007.04.011

[31] R. El-Mallawany, H. Afifi, M. El-Gazery, A. Ali, Effect of Bi2O3 addition on the ultrasonic properties of pentaternary borate glasses, Measurement, 116 (2018) 314-317. https://doi.org/10.1016/j.measurement.2017.11.028

[32] C. Eevon, M. Halimah, Z. Azmi, C. Azurahanim, Elastic properties of TeO_2-B_2O_3—ZnO-Gd_2O_3 glasses using non-destructive ultrasonic technique, Chalcogenide Lett., 13 (2016) 281-289.

[33] M. Elokr, Y. Abou Deif, Optical, elastic properties and DTA of TNZP host tellurite glasses doped with Er^{3}+ ions, J. Mol. Struct., 1108 (2016) 257-262. https://doi.org/10.1016/j.molstruc.2015.11.066

[34] H.A. Al-Shamiri, A. Eid, Optical and ultrasonic properties of chromium oxide in sodium zinc phosphate glass, Photon. Optoelectron., 1 (2012) 1-8.

[35] M. Halimah, H. Sidek, W. Daud, H. Zainul, Z. Talib, A. Zaidan, A. Zainal, H. Mansor, Ultrasonic study and physical properties of borotellurite glasses, Am. J. Appl. Sci., 2 (2005) 1541-1546.

[36] H. Sidek, S. Rosmawati, B. Azmi, A. Shaari, Effect of ZnO on the thermal properties of tellurite glass, Adv. Condens. Matter. Phys., 2013 (2013) 6.https://doi.org/10.1155/2013/783207

[37]A. Abd El-Moneim, I. Youssof, L. Abd El-Latif, Structural role of RO and $A_{l2}O_3$ in borate glasses using an ultrasonic technique, Acta Mater., 54 (2006) 3811-3819. https://doi.org/10.1016/j.actamat.2006.04.012